

Combination Frequency Differencing

1
2
3
4
5
6
7
8
9
10
11
12
13
14
15
16
17
18
19
20
21

D R Kuhn
M S Raunak
Computer Security Division
Information Technology Laboratory

R N Kacker
Applied and Computational Mathematics Division
Information Technology Laboratory

December 6, 2021

This publication is available free of charge from:
<https://doi.org/10.6028/NIST.CSWP.12062021-draft>

22

Abstract

23 This paper introduces a new method related to combinatorial testing and measurement,
24 *combination frequency differencing* (CFD), and illustrates the use of CFD in machine learning
25 applications. Combinatorial coverage measures have been defined and applied to a wide range
26 of problems, including fault location and for evaluating the adequacy of test inputs and input
27 space models. More recently, methods applying coverage measures have been used in
28 applications of artificial intelligence and machine learning, for explainability and for analyzing
29 aspects of transfer learning. These methods have been developed using measures that depend on
30 the inclusion or absence of t -tuples of values in inputs, training data, and test cases. In this paper,
31 we extend these combinatorial coverage measures to include the frequency of occurrence of
32 combinations. Combination frequency differencing is particularly suited to AI/ML applications,
33 where training data sets used in learning systems are dependent on the prevalence of various
34 attributes of elements of class and non-class sets. We illustrate the use of this method by
35 applying it to analyzing physically unclonable functions (PUFs) for bit combinations that
36 disproportionately influences PUF response values, and in turn provides indication of the PUF
37 potentially being more vulnerable to model-building attacks. Additionally, it is shown that
38 combination frequency differences provide a simple but effective algorithm for classification
39 problems.

40

Keywords

41 combinatorial coverage; combination frequency difference; combinatorial testing; physical unclonable
42 function (PUF); unclonable.

43

Acknowledgments

44 The authors are very grateful to Charles Prado of INMETRO Brazil for data used in the PUF analysis and
45 to Sandip Kundu and Vinay Patil for helpful discussion. The authors also plan to continue working with
46 INMETRO to apply and develop these ideas for practical application to PUFs.

47

Disclaimer

48 Any mention of commercial products or reference to commercial organizations is for information only; it
49 does not imply recommendation or endorsement by NIST, nor does it imply that the products mentioned
50 are necessarily the best available for the purpose.

51

Additional Information

52 For additional information on NIST's Cybersecurity programs, projects and publications, visit the
53 [Computer Security Resource Center](#). Information on other efforts at [NIST](#) and in the [Information](#)
54 [Technology Laboratory](#) (ITL) is also available.

55

Public Comment Period: *December 6, 2021 through February 7, 2022*

56

National Institute of Standards and Technology

57

Attn: Computer Security Division, Information Technology Laboratory

58

100 Bureau Drive (Mail Stop 8930) Gaithersburg, MD 20899-8930

59

Email: cfdwp@nist.gov

60

All comments are subject to release under the Freedom of Information Act (FOIA).

61 1 Introduction

62 Methods and tools for measuring combinatorial coverage were initially developed to analyze the degree to which
63 test sets included t -way combinations of values (for some specified level of t) [1][2][4] and have since been
64 studied extensively in the realm of system and software testing [7][8][9][10][11]. Combinatorial coverage
65 measures have been defined and applied to a wide range of problems, specifically for fault location and for
66 evaluating the adequacy of test inputs and input space models. More recently, coverage measures have been used
67 for explainability in artificial intelligence and machine learning [24][28] and for analyzing aspects of transfer
68 learning [27]. These methods have been developed using measures that depend on the inclusion or absence of t -
69 tuples of values in inputs and test cases. For software testing, primarily for deterministic systems where the
70 presence of a particular combination always triggers a specified error, it is relevant whether a t -tuple of values
71 is present in test inputs, but the number of occurrences of a particular t -tuple of values is generally not relevant
72 to testing. Multiple occurrences are only redundant and do not add value. These measures can also be applied in
73 artificial intelligence and machine learning (AI/ML) systems.

74 For many aspects of assurance of autonomous systems and machine learning, this type combinatorial coverage
75 measure is valuable and possibly essential, since the correct and safe behavior of many AI systems is dependent
76 on the training inputs. Conventional structural coverage measures are not applicable to such black box behavior.
77 Consequently, it is essential to evaluate the degree to which possible combinations of input attribute values have
78 been included in training and test sets for AI and autonomy. (Attributes in a machine learning setting correspond
79 to parameters in a test effort; they are the inputs to the system.) If the system has not been shown to function
80 correctly for an input combination that may be encountered in use, then assurance is inadequate. However, for
81 some questions in machine learning, consider the frequency (or rate) of occurrence of t -tuples of values in input
82 and how two different sets may compare or differ in combinatorial coverage.

83 This paper applies combinatorial coverage measures from [13], which include the frequency of occurrence of
84 combinations, in an approach referred to as *combination frequency differencing* (CFD). This method is
85 particularly suited to AI/ML applications, where training data sets used in learning systems are dependent on the
86 prevalence of various attributes of elements of class and non-class sets. This paper illustrates the use of this
87 method by applying it to analyzing physical unclonable functions (PUFs) for potential weaknesses in design and
88 showing how it can be extended to develop a simple but effective classification algorithm.

89 2 Combinatorial Coverage and Combination Frequency Differences

90 This section reviews the basic measures of combinatorial coverage and applications of these measures
91 in Section 2.1. This idea is extended to measures that include the frequency of occurrence of
92 combinations in Section 2.2. These measures can then be applied to the analysis of PUFs.

93 2.1 Basic Combinatorial Coverage and Coverage Difference Measures

94 Combinatorial methods offer an approach to coverage measurement that provides a measure directly related to
95 fault detection. A series of studies have shown that most software bugs and failures are caused by one or two
96 parameters and progressively fewer by three or more [19][20][21][22][5][6]. This finding means that testing
97 parameter combinations can provide more efficient fault detection than conventional methods. This section,
98 derived from [13], reviews the concept of measuring the combinatorial coverage of an input space [1][2][4] for
99 use in testing or in other applications where it is important to ensure the inclusion of combinations of input
100 parameter values.

	a	b	c	d
1	0	0	0	0
2	0	1	1	0
3	1	0	0	1
4	0	1	1	1

101 **Figure 1. Example test array for a system with four binary components**

102 Combinatorial coverage measurement concepts can be illustrated using the example in Figure 1, which shows a
 103 test array that contains 19 of a possible set of 24 2-tuples of values. To facilitate discussion, it is helpful to
 104 establish terminology for two related but distinct concepts:

- 105 • *t-way combination*: a set of t parameters or variables. For example, using the parameters in Figure 1,
 106 (b,d) is a 2-way combination, (a,c) is a different 2-way combination, and (a,c,d) is a 3-way combination.
- 107 • *t-tuple of values*: a combination for which the parameters have specific values. (Note: in the original
 108 definition from [1], this is referred to as a variable-value combination.) For example, $(b=0, d=0)$ is one
 109 t -tuple of values, and $(b=1, d=0)$ is a different t -tuple of values for the same 2-way parameter
 110 combination.

111 A simple combinatorial coverage of t -way combinations, S_t , is the fraction of possible t -tuples of values included
 112 in a test array from a domain D_t that may include constraints. With no constraints, where v is the number of
 113 values and k is the number of parameters, the size of the domain is $v^t \binom{k}{t}$ but may be smaller with constraints.

114 For a set of t -tuples of values A_t in a test array,

115
$$S_t = \frac{|A_t|}{|D_t|}$$

116 **Example:** Figure 1 contains 19 different 2-way combinations out of a possible domain of $2^2 \binom{4}{2} = 24$ t -tuples
 117 of values, so $S_t = 19/24 = 0.79$.

118 Combinatorial coverage differences have been applied to several problem domains. Initially, this approach was
 119 used in fault identification, specifically to determine the particular combination(s) of parameter values that would
 120 trigger a fault. Another example problem where there is a need to distinguish one class of elements from another
 121 is anomaly-based intrusion detection, which seeks to determine if a particular exchange of packets represents an
 122 attempted network intrusion. Thus, it is useful to generalize the approach to find combinations that are present
 123 in one class or set and absent or rare in another, as well as to distinguish one set from another.

124 For fault location, if $A_t =$ the set of t -tuples of values from passing tests and $B_t =$ the set of t -tuples of values
 125 from failing tests, then the set difference $B_t \setminus A_t$ is of interest. These are the combinations in failing tests but not
 126 in passing tests, and thus, those that triggered a failure are contained in this set difference [26].

127 **Example:** If test #2 from Figure 1 is a failing test, then $B_t \setminus A_t = \{bc = 10, cd = 10\}$ is to be investigated to
 128 identify failing combinations because the four other 2-way t -tuples of values in test #2 are also contained in the
 129 passing tests #1, #3, #4, which are set A_t .

130 For transfer learning, if $A_t =$ the set of t -way t -tuples of values from a source set of class instances and $B_t =$ the

131 set of t -tuples of values from a target set of instances, then the size of the set difference $B_t \setminus A_t$ as a fraction of
 132 the target set size is of interest as a metric of how similar the source is to the target set [27]. This set difference
 133 of t -tuples of values is: $\frac{|B_t \setminus A_t|}{|B_t|}$

134 2.2 Distinguishing Combinations

135 For many machine learning applications, the goal is to develop a model that distinguishes members of one class
 136 from another using attributes that identify them, such as distinguishing dogs from cats using attributes like size,
 137 ear shape, or hair texture. This publication will refer to sets being distinguished as either *Class* or *Non-class* sets.
 138 The terms Class and Non-class are used as generic terms for sets of objects that can be distinguished based on
 139 some attributes or properties. In a machine learning context, these sets may refer to concepts that are to be
 140 learned, such as distinguishing one animal species from others. In earlier applications, set differences of t -tuples
 141 of values have been used to identify the causes of failures [4][5]. In both cases, the process is the same – set
 142 differencing is used to identify combinations that occur in the class set that do not occur, or are rare, in the non-
 143 class set. If this difference is computed on t -tuples of values in failed tests versus passed tests, then the difference
 144 contains t -tuples of values that have triggered the failure (in a deterministic system). In machine learning, the
 145 difference represents properties or attributes that occur in the class (e.g., a particular animal species) that do not
 146 occur, or are rare, in the non-class examples (other species). Note that this is simply a generalized version of the
 147 original fault location problem, where the class whose distinguishing features are to be identified is the set of
 148 failing tests, and the features to be found are the combinations that lead to a test resulting in a failure.

149 The combinatorial coverage measures described in the previous section – as applied in fault location,
 150 explainability, and transfer learning – are based on the presence or absence of t -tuples of values in input files for
 151 testing or machine learning training. That is, a combination is counted as covered if it occurs once or multiple
 152 times in the input file, and this measure is appropriate in the applications discussed. For these applications, it is
 153 important to determine if a t -tuple of values has been included, but the number of times it occurs is less important.
 154 For testing, multiple occurrences of a combination mean some duplication of effort but do not affect the
 155 requirement for ensuring that all t -way combinations have been covered. In transfer learning evaluation, the
 156 same type of requirement holds – assurance that states and environments, as represented by t -tuples of values of
 157 the input model, are handled correctly. If it can be shown that the ML model produces the right prediction or
 158 classification for a t -tuple of values, multiple occurrences of the combination are not needed. (This does not
 159 consider the effect of input sequences; other measures are appropriate for sequence coverage.)

160 In other types of evaluations related to machine learning, it will be important to consider the number or frequency
 161 of occurrence of t -way t -tuples of values to determine the degree to which an attribute is associated with a
 162 particular class. If a particular combination of attribute values is seen in a high proportion of class members but
 163 not in non-class members, then it may be a reasonable indicator for distinguishing instances or at least for
 164 narrowing the range of possibilities for class identification. For example, many dog breeds may have a long tail,
 165 and many may have a curled tail, but a much smaller number of breeds have both attributes. Thus, it is important
 166 to have a measure that considers the quantity of instances with t -tuples of values in class and non-class instances.

167 This paper will abbreviate C_t and N_t as C and N , where interaction level t is clear or is not needed for discussion.
 168 The following discussion defines a t -way combination c_t as a distinguishing combination for the class C if it is
 169 present in a class instance of class set C and absent in non-class instances N , or if it is more common in C than
 170 N as determined by a threshold value. Two ways to identify distinguishing combinations are suggested below,
 171 and others are clearly possible. The key point is to use combinations of attribute values that are *strongly*
 172 *associated* with one class but not with others based on the frequency or rate of occurrence in one class as
 173 compared with others.

174 At least two possible ways to define the strength of association of a t -tuple of values with a class can be
 175 considered. These are defined and presented below as CFD1 and CFD2. (In a previous publication, only CFD1
 176 was given as the definition of this strength of association [13].) The threshold T in definition CFD1 determines
 177 if a t -tuple of values c_t is common in set C_t and rare in set N_t and, thus, distinguishes one set from the other.
 178 Specifically, the definition below identifies t -tuples of values for which one can say “ x is T times more common
 179 in C than it is in N ” – an intuitive way to identify t -tuples of values that are associated closely with the class C .
 180 Note that the phrase “ T times more common” suggests that T will normally be 1 or greater. For definition CFD2,
 181 U designates the threshold value. T may be any positive number, and U ranges from 0.0 to 1.0. Notice that these
 182 definitions produce the same result for inclusion or exclusion in the set of distinguishing combinations when
 183 $T = \frac{1}{1-U}$, or $U = \frac{T-1}{T}$. For example, if $T = 4$ or $U = 0.75$, then for pairs $[(f(x_t, C_t) ; f(x_t, N_t))]$, $[\cdot 81 ; \cdot 2]$, and $[\cdot 79 ;$
 184 $\cdot 2]$, the first will be found to be distinguishing, and the second will not.

185 CFD1 Definition: A combination x_t is *distinguishing* for a class $C \Leftrightarrow f(x_t, C_t) > T \times f(x_t, N_t)$, where $f(x_t, Y_t)$
 186 = frequency of t -tuple of values x in set of t -tuples of values Y . The frequency f is the number of times a t -tuple
 187 of values appears in rows of the class over the number of rows for the class.

188 CFD2 Definition: A combination x_t is *distinguishing* for a class $C \Leftrightarrow \frac{f(x_t, C_t) - f(x_t, N_t)}{f(x_t, C_t)} > U$, where $f(x_t, Y_t) =$
 189 frequency of t -tuple of values x in set of t -tuples of values Y . Note that, in this case, the threshold U ranges from
 190 0.0 to 1.0. The frequency f is the number of times a t -tuple of values appears in rows of the class over the number
 191 of rows for the class.

192 The choice of CFD1 or CFD2 as a definition may depend on which is more intuitive for the application.
 193 Specifying $T = 1$ or $U = 0$ means that a combination is selected as distinguishing whenever it occurs at a higher
 194 frequency in C than N , no matter how small the difference in frequency.

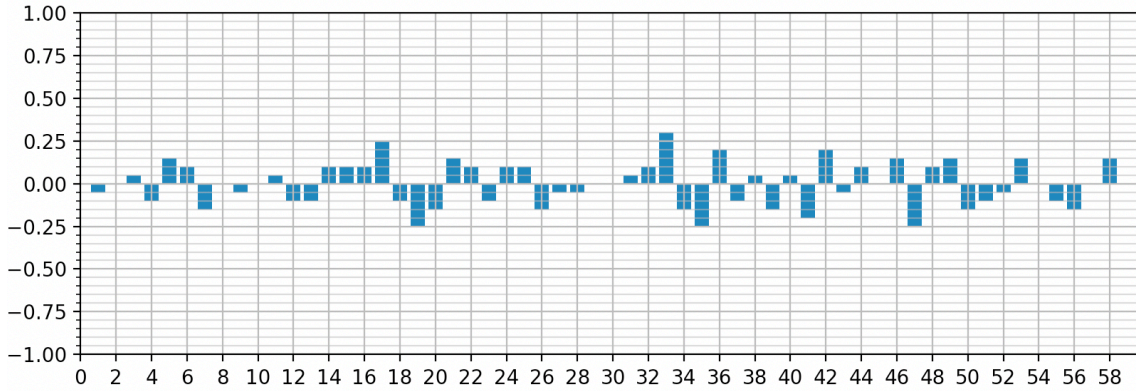
195 2.3 Combination Frequency Difference Measures

196 The frequency (or rate) of occurrence refers to the number of times a t -tuple of values is present per number of
 197 rows in the file or array. Therefore, the combination frequency difference, for a t -tuple of values x in two arrays
 198 of instances of two different classes can be defined as the difference between the fraction of occurrences in one
 199 array and the second. That is, using the symbols defined below, $CFD = F_{Cx} - F_{Nx}$, where

- 200 R = number of rows of challenge-response file
- 201 R_C = rows of class instances; for PUFs, $R_C = R_l$ (i.e., where challenges produce a 1 response)
- 202 R_N = rows of non-class instances; for PUFs, $R_N = R_0$
- 203 k = number of columns or attributes, excluding class or response variable; for PUFs, $k = 64$
- 204 v = number of values for attributes; for PUFs, $v = 2$ as the attributes correspond to bits
- 205 M_{Cx} = number of occurrences of a particular t -tuple of values x in C
- 206 M_{Nx} = number of occurrences of a particular t -tuple of values x in N
- 207 $F_{Cx} = M_{Cx}/R_C$ = fraction of occurrences of a t -tuple of values in C
- 208 $F_{Nx} = M_{Nx}/R_N$ = fraction of occurrences of a t -tuple of values in N

209 The frequency difference values can be graphed, where the height on the Y axis shows the difference $F_{Cx} - F_{Nx}$
 210 for every t -tuple of values x . The X axis is indexed by $v^t \binom{k}{t}$, points for t -way combinations. Thus, for each t -
 211 way combination, there are v^t possible values or settings of the t attributes or variables in the combination. For
 212 example, 2-way t -tuples of values are displayed in the order given by: i, j for i in $0 \leq i < k-1$ for j in $i+1 \leq j < k$.
 213 Thus, there are $k-1$ iterations of the inner loop on j for each attribute i , and for each 2-way combination, the

214 graph displays the fraction of occurrences of each set of v^2 t -tuples of values on the X axis at
 215 $v^2((k-1)i + j - 1)$ through $v^2((k-1)i + j - 1) + v^2 - 1$. For each of these 2-way combinations x , F_{Cx} -
 216 F_{Nx} for four t -tuples of values are displayed for the four possible value settings 00, 01, 10, 11. Thus, in Figure
 217 2, the difference in coverage for C and N for $i=1, j=4$ will be found on the horizontal axis at $x = 32..35$.
 218



219
 220 **Figure 2. Example combinatorial frequency difference for two classes of 6 binary variables**

221 For example, with $n = 6$ numbered 0..5, 2-way combinations will be indexed on the Y axis as (0,1,00),
 222 (0,1,01),..., (4,5,11), for a total of $2^2 \binom{6}{2} = 60$ X-axis points, numbered 0..59. For each of these, the Y-axis
 223 shows the difference in frequency of occurrence between C and N, normalized for the size of sets C and N. For
 224 example, if the value 01 for attribute combination $i=1, j=4$ occurs 40 times in a C file of 100 rows and 60 times
 225 in an N file of 120 rows, then the Y axis value for $i, j = 1, 4$ for value 01 is $(40/100) - (60/120) = -0.1$. The analysis
 226 of PUFs described in this paper can use these quantities to identify bits related to internal structure.

227 **3 Application to Physical Unclonable Functions**

228 A physical unclonable function, or PUF, may be regarded as a physical implementation of a black box function
 229 that produces a response r for a given challenge string of bits c , that is, $r = f(c)$. The unit response is binary and
 230 can be represented as 0 or 1. A series of PUFs can be put together to produce a larger response sequence. As the
 231 name suggests, PUFs are designed using physical hardware devices. These functions utilize unique properties of
 232 the physical elements within the hardware, such as the small variation in propagation delays between identical
 233 circuit gates or small threshold mismatches in a transistor feedback loop due to process variation. These physical
 234 characteristics are difficult to reproduce in the hardware, which is what makes them physically unclonable. Using
 235 such physical characteristics, PUFs can be utilized to combat insecure storage, hardware counterfeiting, and
 236 other security problems.

237 An ideal PUF should be stable over time, unique in its existence, easy to evaluate, and difficult or impossible to
 238 predict. Thus, it should not be possible to generate a function that has the same behavior or produces the same
 239 output as the PUF for challenge inputs. In this sense, the PUF function is “unclonable.” It should also be
 240 infeasible to determine components of the PUF that influence the output of the PUF, such that a 0 or 1 value in
 241 some positions of the input string makes a 0 or 1 output more likely for the output r .

242 The primary use of PUFs is related to authentication. In a simple use case, the physical system is subjected to

243 one or more challenges during manufacturing, and the responses to these challenges are recorded. Later, if one
 244 of those recorded challenges is repeated and if the expected response is received, then the device is authenticated.

245 Depending on the strength of their implementation and consequent scalability, PUFs are categorized into two
 246 levels – weak and strong. Weak PUFs have a limited number of challenge-response pairs (CRPs) that can be
 247 generated from a single device, while strong PUFs can generate a much larger set of CRPs. One of the key
 248 requirements for a strong PUF design is that it should not be possible to infer information about the internal
 249 structure by observing inputs and outputs [16]. Many authors have shown that machine learning models can be
 250 constructed to predict the output of PUFs for a given input string (i.e., “breaking” the PUF by defeating its
 251 authentication function). Vulnerability to breaking through machine learning attacks can vary significantly with
 252 PUF design, and one of the challenges in developing PUFs is to identify potential weaknesses before constructing
 253 the PUF.

254 Table 1 shows ML prediction results for the five PUF designs discussed in this paper and for 10 ML algorithms
 255 available through the Weka machine learning tool package [17]. Note that ZeroR is a baseline, where predictions
 256 are simply the proportion of 0 or 1 results for the challenge/response pairs in the training set. The other algorithms
 257 were selected to provide a representative sample of popular ML algorithms of different types. AdaBoost is an
 258 adaptive ensemble algorithm that uses a phased sequence of basic decision tree algorithms, improving on
 259 prediction results with each phase. Bayes Net and Naïve Bayes are based on Bayesian statistical concepts.
 260 Decision Table is a majority classifier based on a nearest neighbor algorithm. J48 and Random Forest are based
 261 on decision trees. Stochastic gradient descent minimizes a loss function that is a weighted linear combination of
 262 the attributes, and logistic regression uses weighted attributes in a regression function. JRip is a propositional
 263 logic-based rule learning algorithm. Although there is a wide range of results for different algorithms, it is clear
 264 that DB1 – the arbiter design – is much more vulnerable to ML attacks, where two algorithms are able to predict
 265 the response to challenges with near perfect accuracy. Even the best two PUF implementations (DB3 and DB4)
 266 are not fully resistant to revealing some bias in their responses. Note that their averages are all considerably
 267 above the baseline ZeroR, which simply guesses in proportion to 0 or 1 responses in challenge-response pairs.

268 **Table 1. ML Prediction results for five PUF designs**

	Ada Boost	BayesNet	Decision Table	J48/C45	JRip	Logistic	Naïve Bayes	Random Forest	Stoc Grad Descent	ZeroR	Average accuracy	combined diff 2-way
DB1	77.1	96.2	75.6	72.1	77.2	99.7	96.2	87.2	99.3	55.0	86.7	0.489
DB2	54.8	54.9	76.7	68.1	75.2	54.9	54.9	71.9	52.4	55.6	62.6	0.309
DB3	50.7	50.1	71.0	63.9	67.2	50.3	50.1	62.6	50.2	50.1	57.3	0.248
DB4	57.5	56.5	58.8	54.6	60.7	56.4	56.5	55.3	54.6	50.6	56.8	0.216
NN00	64.1	64.8	62.1	59.1	64.8	64.8	64.8	65.4	62.6	50.5	63.6	0.383

269 This section shows how combination frequency differences of PUF input data can be used to determine a good
 270 deal of information about the design and internal structure of a PUF. This is achieved by measuring the difference
 271 between occurrences of *t*-way combinations associated with a 0 response as compared with a 1 response. Ideally,
 272 there should be little difference, except for random variances. As shown below, however, these differences vary
 273 considerably and align with the differences in predictability using machine learning. Although this work is only
 274 preliminary, this information may be useful in identifying design deficiencies and making PUFs more resistant
 275 to breakthrough machine learning.

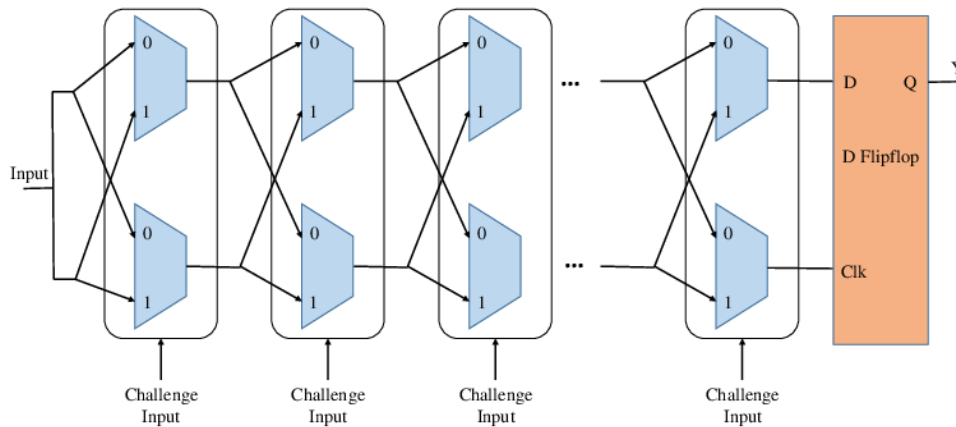
276 Comparing the accuracy of ML predictions in Table 1 with the graphs in Figures 3 through 7, it is immediately
 277 apparent that there is a relationship between the “noisiness” of the graphs and the success of ML algorithms in
 278 predicting or breaking the PUF. The arbiter PUF, DB1 (Figure 3), response has a very noisy graph with

279 differences for nearly every 2-way combination of bits ranging from about 0.10 to 0.25. For this PUF, ML
 280 algorithms predict the response with up to 99.7 % accuracy. For the PUF most resistant to ML predictions, DB4
 281 (Figure 6), the graph shows small frequency differences with nearly all under 0.05 and up to a few around 0.10.
 282 The others fall within the range between DB1 and DB4 for both frequency differences and prediction accuracy,
 283 which is a metric for the potential of breaking the PUF. Maximum frequency differences for DB3 are around
 284 0.12, for DB2 about 0.15, and for the neural net PUF around 0.19 – roughly consistent with the rankings of best,
 285 worst, and average for prediction accuracy and, hence, vulnerability to ML attacks. See the last column of Table
 286 1, which shows the range for 2-way frequency differences above and below the center line, or $\max(|f(x_i, C_t) -$
 287 $f(x_i, N_t)|) + \max(|f(x_i, N_t) - f(x_i, C_t)|)$.

288 There are two major types of hardware implementation of PUFs: memory-based and delay-based. A typical
 289 memory-based PUF is the SRAM PUF. Delay-based PUFs include arbiter PUFs, the pseudo-linear feedback
 290 shift register PUF, and the ring oscillator (RO) PUF.

291 3.1 Arbiter PUF (DB1)

292 The main idea of an arbiter PUF is to create a digital race for signals through two paths within a chip and to have
 293 an *arbiter* circuit that decides which signal has won the race. The two paths are designed identically. However,
 294 the manufacturing process usually introduces a very slight longer delay in one of the paths from the other. Given
 295 a particular challenge, the arbiter PUF will therefore produce an output dictated by the physical characteristics
 296 of that unique hardware implementation. During an arbiter PUF design, one has to make sure that the delays
 297 between the two paths are not too close to each other. Otherwise, the output will be dictated by noise in the signal
 298 rather than the delay uniquely introduced through the manufacturing variation.



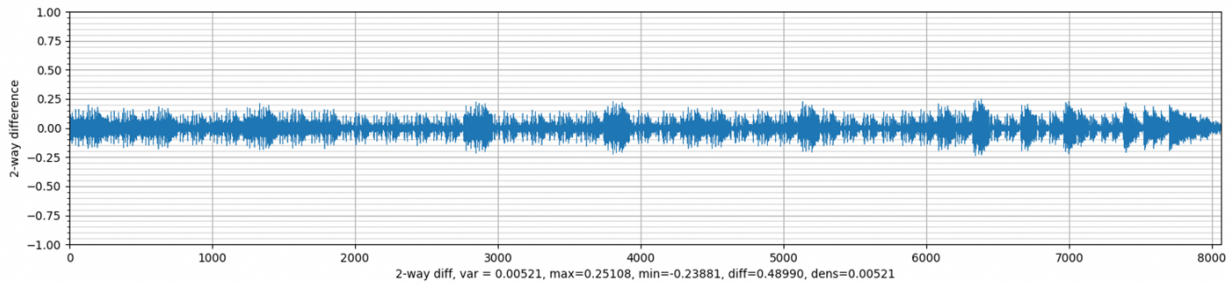
299
 300 **Figure 3. Basic operations of an arbiter PUF**

301 As Figure 3 shows, each gate or switch-block introduces a delay for one of the outputs, which accumulates over
 302 the blocks. This gives rise to the opportunity of building what is typically known as *model-based attacks* (also
 303 known as *model building attacks* or *model learning attacks*). The idea is that one can build a mathematical model
 304 of the PUF which, after observing several CRP queries, will be able to predict the response for a given challenge
 305 with a high level of accuracy. With the proliferation of machine learning algorithms, this type of model building

306 or model learning has become easier to implement. To make model building attacks more difficult on basic
 307 arbiter PUFs, non-linearity is introduced into the delay lines of the designed circuit. For example, in case of feed-
 308 forward arbiter PUFs, some challenge bits are not set by the user. Rather, they are connected to the outputs of
 309 the intermediate arbiters evaluating the race at some intermediate point the circuit. This technique, however,
 310 increases the noise in the output of the arbiter PUF. Although initial results with feed-forward arbiter PUFs were
 311 shown to be resistant to model-building or model-learning attacks, more sophisticated learning models were able
 312 to break them [17].

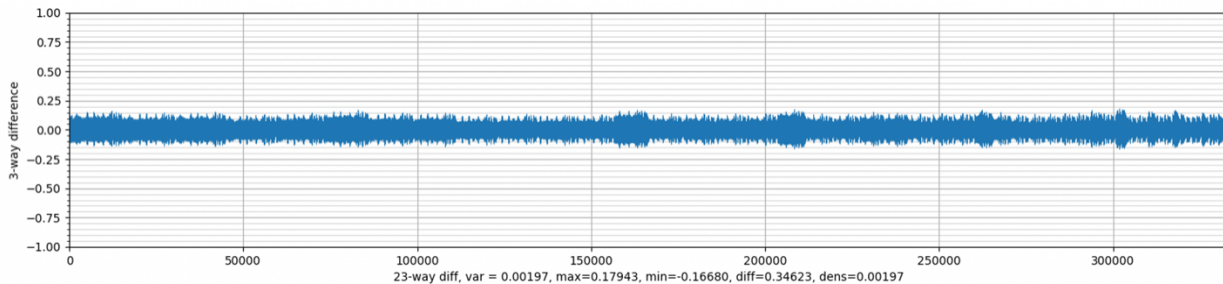
313 By simply analyzing combination frequency differences (CFD) within a subset of the challenge-response pairs
 314 (CRPs) and without knowing anything about the type or design of the circuitry, one can predict which arbiter
 315 PUF design is likely to be more vulnerable to model-building attacks.

316 Figure 3(a) shows 2-way frequency differences for a 64-bit PUF, DB1, an early arbiter design with delays placed
 317 randomly in the hardware. With 64 bits, there are $2^2 \binom{64}{2} = 8064$ 2-way differences indexed. Differences range
 318 from a low of -0.23881 to a high of 0.25108 for a range of 0.48990. Note that differences are given as difference
 319 $F_{C_x} - F_{N_x}$, so negative values are cases where non-class t -tuples of values exceed class t -tuples of values.



320
 321 **Figure 3(a). 2-way frequency differences for a 64 bit arbiter PUF**

322 Figure 3(b) shows 3-way frequency differences for the same PUF. Note that variance, minimum, and
 323 maximum differences are smaller than those for 2-way combinations. The X axis indexes $2^3 \binom{64}{3} = 333,312$
 324 combinations.



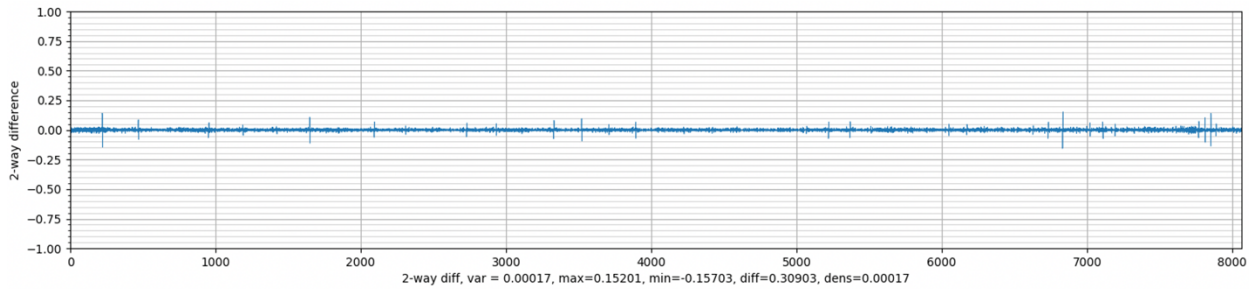
325
 326 **Figure 3(b). 3-way frequency differences for a 64 bit arbiter PUF**

327 **3.2 8-bit Shift Register PUF (DB2)**

328 Shift register PUF is another delay-based PUF implementation, where a series of linear feedback shift registers

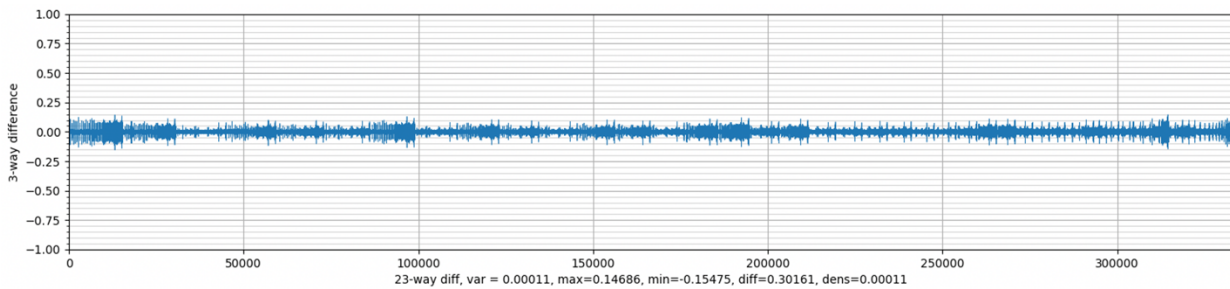
329 (LFSR) are put together to capture the unique delays associated with a physical implementation. Researchers
330 have proposed pseudo-LFSR-based physically unclonable functions, known as PL-PUF, which are usually small
331 in size, efficient in producing authentication ID for devices, and easy to modify to adjust the challenge-response
332 pairs when needed [29].

333 This section examines the security of a shift register-based PUF against a model-based attack using combinatorial
334 frequency difference analysis. Frequency differences for an 8-bit shift register type of PUF are shown in Figure
335 4(a) (2-way) and Figure 4(b) (3-way). Note that the variance is much smaller – 0.00017 compared to 0.0521 for
336 2-way combinations of DB1 inputs. There is much more uniformity in the response of DB2 to 2-way and 3-way
337 combinations of input bits, and as expected, this makes it much more difficult for ML to derive a model for the
338 PUF that can successfully reproduce its response to inputs.



339

340 **Figure 4(a). 2-way frequency differences for an 8-bit shift register PUF**



341

342 **Figure 4(b). 3-way frequency differences for an 8-bit shift register PUF**

343 However, Figure 3(a) also shows a small number of spikes in the combination frequency chart. Combinations
344 producing these spikes are shown in Table 2, which shows 2-way bit combinations where the frequency
345 difference exceeds 3σ . Combinations of almost all bits with bit 56 result in a spike that exceeds 3σ (others have
346 spikes that are slightly below this value but still clearly different from the other combinations). The appearance
347 of spikes compresses towards the right end of the graph because combinations are indexed in a loop computation:
348 i, j, b : for i in $0 \leq i < 63$ for j in $i+1 \leq j < 64$ for b in $\{00,01,10,11\}$, similarly for 3-way combination indexes.

349

350

351

Table 2. 2-way combinations with greatest frequency differences in Figure 4(a)

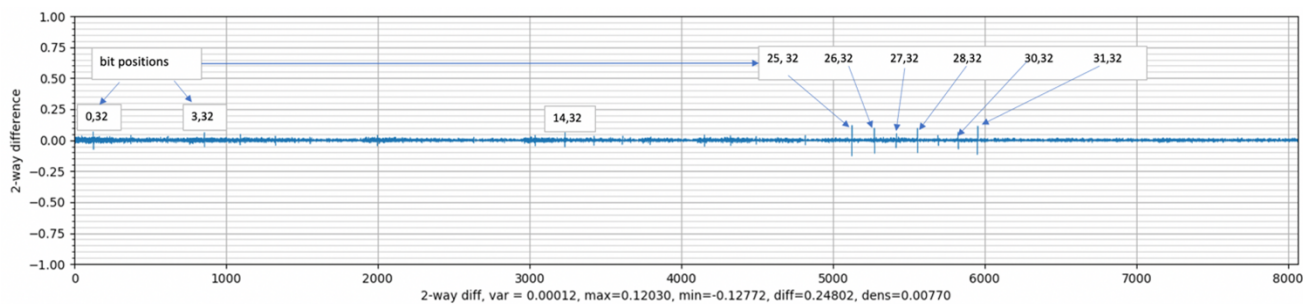
bits = values	bits = values	bits = values	bits = values
(0,56) = (1,0)	(11,56) = (0,0)	(26,56) = (1,1)	(41,56) = (0,1)
(0,56) = (0,1)	(12,56) = (1,0)	(26,56) = (0,0)	(42,56) = (1,1)
(1,56) = (1,0)	(12,56) = (0,1)	(31,56) = (1,1)	(42,56) = (0,0)
(1,56) = (0,1)	(14,56) = (1,1)	(31,56) = (0,0)	(51,56) = (1,1)
(3,56) = (1,1)	(14,56) = (0,0)	(32,56) = (1,1)	(51,56) = (0,0)
(3,56) = (0,0)	(15,56) = (1,0)	(37,56) = (1,1)	(52,56) = (1,0)
(4,56) = (1,0)	(15,56) = (0,1)	(37,56) = (0,0)	(52,56) = (0,1)
(6,56) = (1,0)	(16,56) = (0,1)	(38,56) = (1,1)	(53,56) = (1,1)
(6,56) = (0,1)	(17,56) = (1,0)	(38,56) = (0,0)	(53,56) = (0,0)
(8,56) = (1,1)	(17,56) = (0,1)	(40,56) = (1,0)	(54,56) = (1,1)
(8,56) = (0,0)	(25,56) = (1,1)	(40,56) = (0,1)	(54,56) = (0,0)
(11,56) = (1,1)	(25,56) = (0,0)	(41,56) = (1,0)	

352 A potential explanation can be developed for the pattern of spikes in combinations that include bit 56 by noting
 353 that 8 is an even divisor of 56. PUFs accumulate differences as steps progress, so bit 56 occurs at the final stage
 354 before the last 8-bit shift register. In a design situation, the next step would be to analyze the hardware
 355 components to determine why this irregularity was occurring.

356 **3.3 32-bit Shift Register PUF (DB3)**

357 This section shows the results of the analysis performed on a 32-bit shift register PUF. As the name suggests, a
 358 32-bit shift register PUF is designed the same as an 8-bit shift register, where the circuitry is four times longer.
 359 The added circuitry increases the complexity of the PUF and, thus, likely makes it a little less susceptible to
 360 model-building attacks.

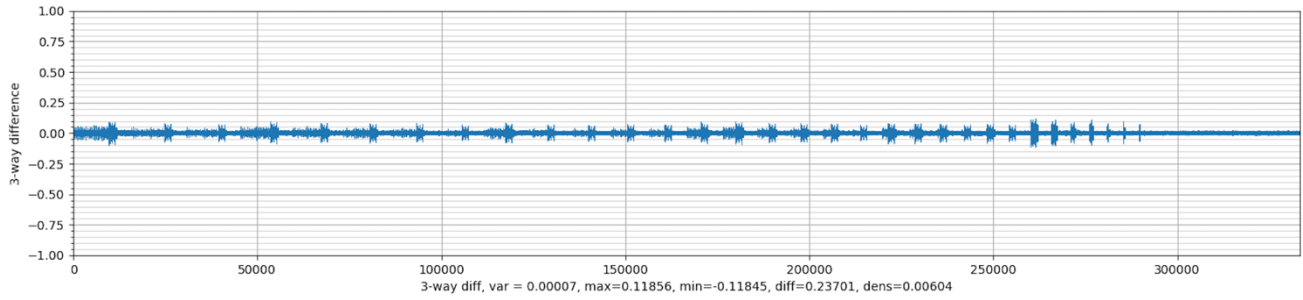
361 The results of applying the analyses are shown in Figures 5(a) and 5(b).



362

363

Figure 5(a). 2-way frequency differences for a 32-bit shift register PUF



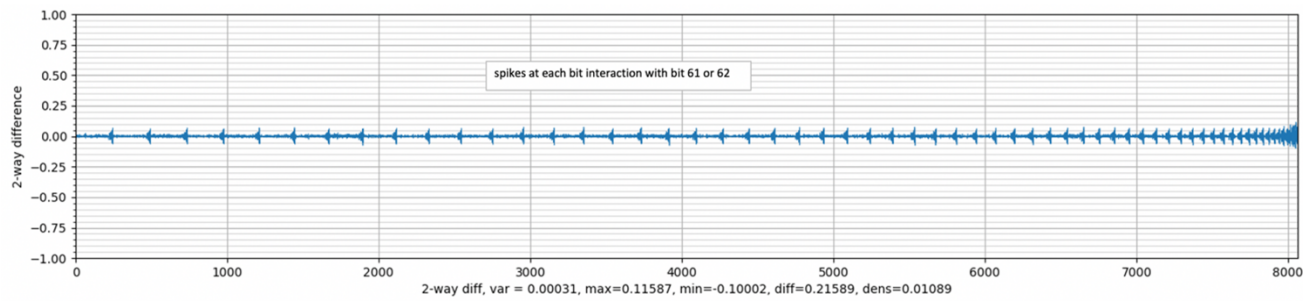
364

365

Figure 5(b). 3-way frequency differences for a 32-bit shift register PUF

3.4 Uniform distribution PUF (DB4)

367 Figure 6 shows results for a PUF with the most uniform distribution of all studied here. This PUF has the greatest
368 resistance to machine learning attacks, which are able to predict responses only somewhat better than chance
369 (see Table 1). In this case, the variations used in producing PUF responses accumulate uniformly with slight
370 frequency differences for t -tuples of bits that include either bit 61 or 62. (Compression of the spikes towards the
371 right side of the graph occurs because of the loop computation, as explained in Section 3.2.)

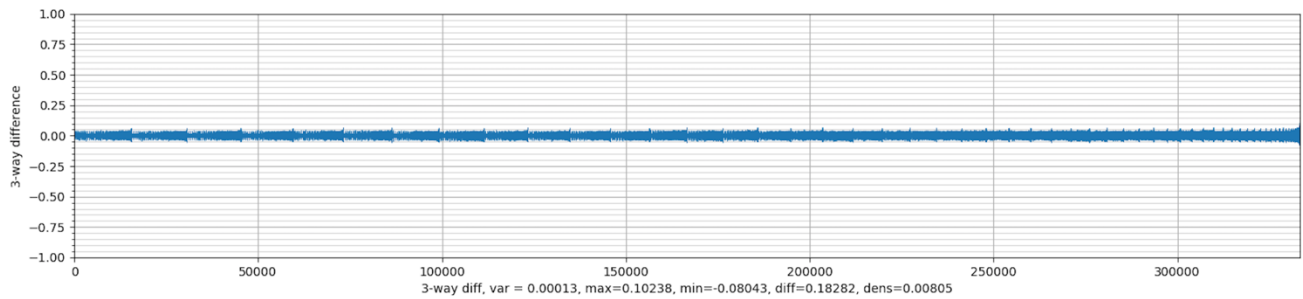


372

373

Figure 6(a). 2-way frequency differences for a uniform distribution PUF

374



375

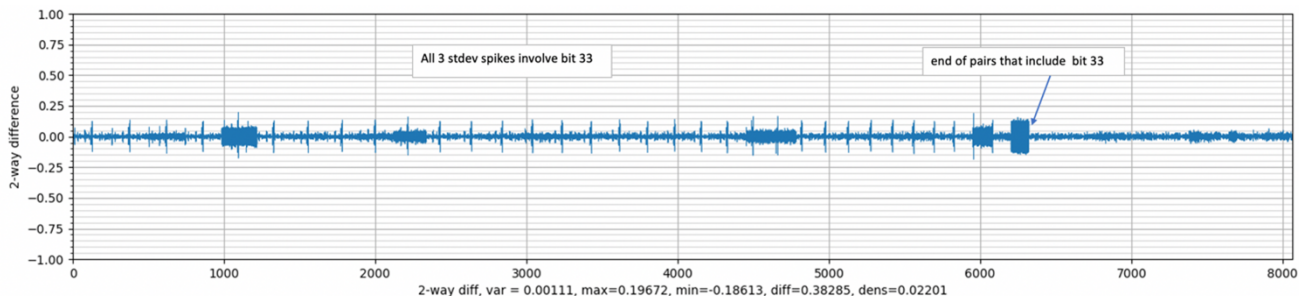
376

Figure 6(b). 3-way frequency differences for a uniform distribution PUF

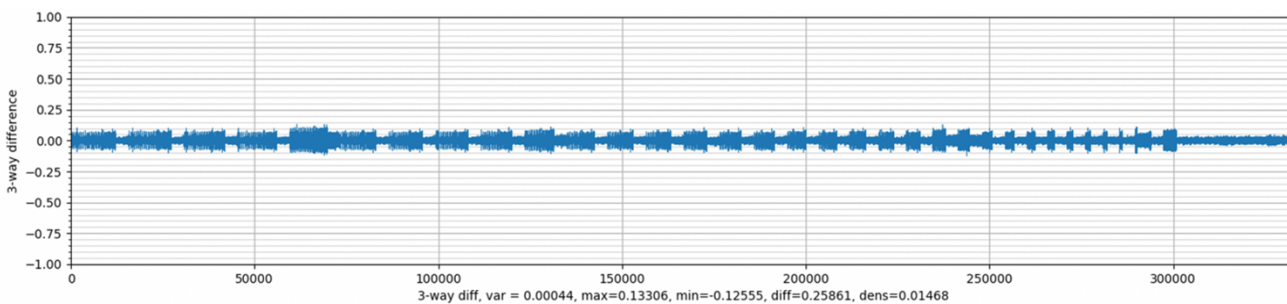
377

378 **3.5 Neural Net PUF**

379 Researchers have pointed out the vulnerabilities of arbiter and other types of PUFs, especially against model-
 380 building attacks [30]. To thwart the model-learning attack, researchers proposed both a simple neural network
 381 (NN) [31] as well as recurrent neural network (RNN)-based PUFs [32]. These new models are specifically
 382 designed for high resistance to model-building attacks achieved by introducing non-linearity between the
 383 challenge-response pairs. The physical implementation uses current-mirrors to construct the PUF. The basic idea
 384 is to propagate a current through two identical chains of non-linear current mirrors. In the case of RNN-based
 385 PUF, the circuitry feeds back the challenge bits into the PUF. [32]



386
 387 **Figure 7(a). 2-way frequency differences for a neural net PUF**



388
 389
 390 **Figure 7(b). 3-way frequency differences for a neural net PUF**

391 **4 Extension to Machine Learning**

392 A *distinguishing combination* has been defined as one present in a class instance of class set C and absent in
 393 non-class instances N , or if it is more strongly associated with C than N , as determined by a threshold value. As
 394 the name suggests, a distinguishing combination is one that differentiates one type or class of instance from
 395 others. Thus, it is natural to consider if these combinations can be used directly in machine learning problems
 396 for predicting class membership from instance attributes. If an instance contains many t -tuples of values that are
 397 associated with a particular class but not with other classes, then it is likely to be a member of the class with
 398 which the t -tuples of values are strongly associated. This section shows that initial results suggest this approach
 399 works quite well in many cases. No ML algorithm is best for all problems, and the CFD approach to classification
 400 performs better than other ML algorithms for some problems and less well for others. This section reviews some
 401 of these empirical results and suggests future work to characterize the conditions under which CFD machine

402 learning will be advantageous.

403 Given a set of distinguishing combinations, a simple algorithm for classification seems natural: if an instance
 404 has more attribute combinations that are associated with a class C than another class, then assign it to C , and if
 405 there are fewer combinations associated with C than another class, then assign it to the other class. (For
 406 simplicity, only two classes are considered here, but the method can be extended to multiple classes by
 407 considering each one as “ C ” in turn). If the C and N combinations are equally present, then the result is
 408 undermined. As the saying goes, “if it looks like a duck and walks like a duck and quacks like a duck (a 3-way
 409 combination), it’s probably a duck!”

410 CFD algorithm:

```

411     dist_c = {distinguishing combinations for instances in class C}
412     dist_n = {distinguishing combinations for instances not in class C}
413
414     dc = sum(1 for t-way combinations  $x_i$  in row if  $x_i$  in dist_c)
415     dn = sum(1 for t-way combinations  $x_i$  in row if  $x_i$  in dist_n)
416     if dc > dn: predict C
417     if dn > dc: predict N
418     if dc == dn: indeterminate
    
```

419 A number of possible alternatives to the basic algorithm can be conceived. Perhaps the most obvious is to weigh
 420 the presence of distinguishing combinations in instances, shown below as CFDw. Using a weight of $|F_{Cx} - F_{Nx}|$,
 421 the CFDw algorithm has been compared with the basic CFD for several examples. Comparisons of the weighted
 422 method with the basic method are shown in the following sections along with frequency difference graphs.
 423 Accuracy scores for CFD and CFDw are relatively close, and there is no clear winner between these two
 424 variations.

425 CFDw algorithm:

```

426     dc = sum(weight( $x_i$ ) for t-way combinations  $x_i$  in row if  $x_i$  in dist_c)
427     dn = sum(weight( $x_i$ ) for t-way combinations  $x_i$  in row if  $x_i$  in dist_n)
428     if dc > dn: predict C
429     if dn > dc: predict N
430     if dc == dn: indeterminate
    
```

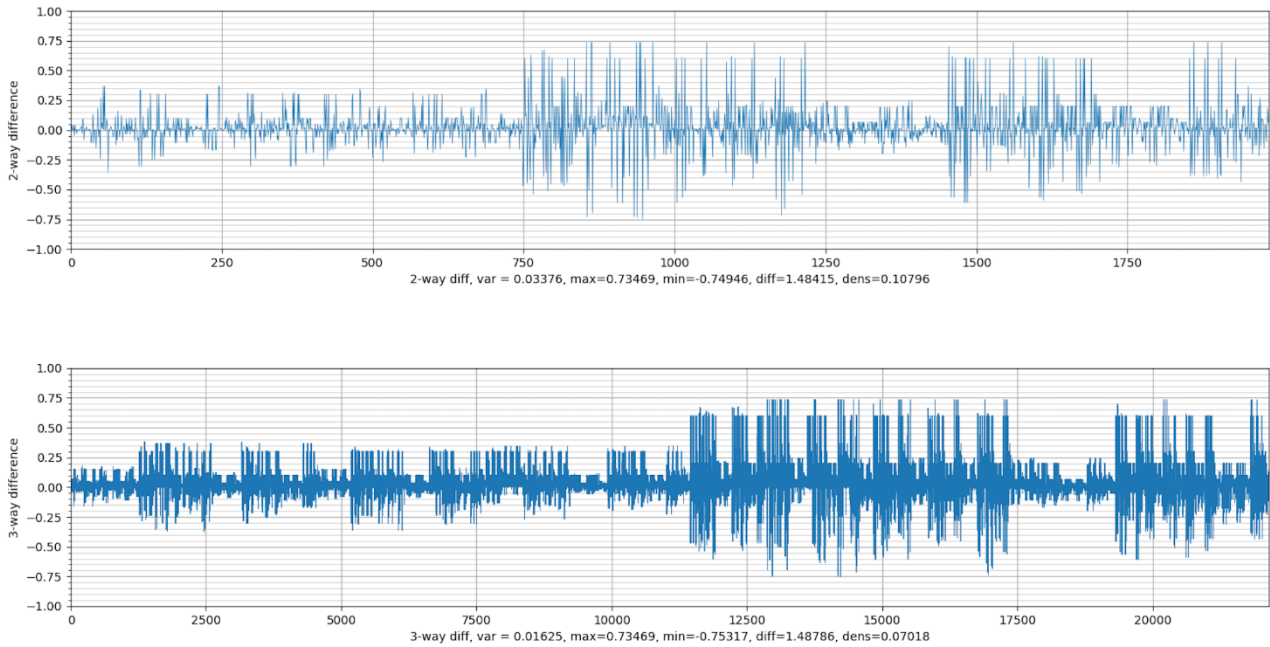
431 Using this approach on the PUF data presented in the previous section produces results that are relatively
 432 comparable to the ML algorithms shown in Table 1 for 10,000 rows using 4-way combinations shown in Table
 433 3.

434 **Table 3. Comparison of CFD accuracy with average, best, worst from Table 1**

	CFD	Avg, Table 1	Best, Table 1	Worst, Table 1
DB1	.953	86.7	.997 (logistic)	.721 (J48)
DB2	.547	62.6	.767 (dec tbl)	.524 (SGD)
DB3	.520	57.3	.710 (dec tbl)	.501 (Bayesnet)
DB4	.546	56.8	.607 (JRip)	.546 (SGD)
NN00	.621	63.6	.654 (Rand Forest)	.591 (J48)

435 As previously discussed, PUFs are designed to be “unclonable” (i.e., difficult to replicate, including through
 436 strategies such as machine learning). In most ML applications, the classes of interest are in nature or may be
 437 industrial products not designed to be resistant to modeling. This difference is also immediately apparent in the
 438 graphs in Appendix A, which show much wider variation for these “natural” or practical datasets. An example
 439 is shown in Figure 8 below (mushroom data set from Appendix):

440



441

442 **Figure 8. Frequency difference graph for 2-way and 3-way differences, mushroom example**

443 As shown in this graph and others in Appendix A, there is a much wider variation in frequency differences – up
 444 to roughly 75 % or more. The much smaller variation for PUFs is likely due to the fact that they are designed
 445 to be difficult to clone or replicate. The wider range of frequency differences in these natural examples make the
 446 CFD approach more effective, using the differences to distinguish between classes. On these applications, CFD
 447 class prediction does quite well, as shown in Table 4. Accuracy scores in the column labeled “CFD4 @ T” are
 448 the average of 10 random assignments of the total number of rows given by “n rows” split into 66 % training
 449 and 34 % test for the threshold of T shown using 4-way combinations.

450

Table 4. Comparison of CFD accuracy with other ML algorithms

Dataset	n row	n col	n class	n non	CFD4 @ T	Ada	Baye	DecTbl	J48	JRip	Log	NB	Rand	SGD	ZR
Bcanc	286	9	68	218	.970@1.0	.759	.766	.745	.769	.720	.752	.752	.745	.766	.762
Coupon	12684	25	7210	5474	.730@5.0	.644	.663	.688	.718	.725	.693	.663	.757	.684	.569
Credit	1000	20	37	963	.991 @ 5.1	.963	.950	.962	.963	.957	.958	.949	.963	.963	.963
Diab	768	8	367	401	.992@1.0	.698	.723	.709	.694	.692	.728	.723	.674	.715	.522
Heart2	47786	21	23893	23893	.755@5.0	.745	.741	.745	.757	.754	.767	.741	.753	.762	.500
Mush	5644	22	2156	3488	1.00 @ 1.0	.963	.985	1.00	1.00	1.00	1.00	.974	1.00	1.00	.618
Soyb	684	31	133	551	.986 @ 15.0	.991	.968	.988	.981	.972	.975	.929	.983		.845

451 It is important to note that a small number of threshold values have been tried. Further experimentation with
452 threshold values and characterization of their applicability will be the subject of future research. An additional
453 issue to be investigated is the possibility of overfitting. Two of the sample machine learning data sets have less
454 than 10 attributes. Using 4-way combinations to test for membership in class or non-class sets may have a
455 potential for overfitting because a 4-way combination could include roughly half of the attributes available for
456 classifying an instance. The other data sets were chosen with more than 20 attributes to reduce the possibility of
457 overfitting. A detailed investigation of this issue will be the subject of future research.

458 **5 Conclusions**

459 This paper presents a method for measuring and visualizing differences in the frequency or rate of occurrence of
460 t-way combinations for two data sets. This measure, combination frequency differencing (CFD), has potential
461 use in a variety of applications. Initially applied to challenge-response pairs for physical unclonable functions of
462 PUFs, CFD was shown to provide the ability to identify combinations of bits in the challenge that are more or
463 less strongly associated with particular output values of 0 or 1. The level of difference appears to correlate with
464 the effectiveness of machine learning attacks on PUFs. In future research, the authors hope to develop ways to
465 trace these strongly non-uniform bit combination associations to the hardware components that produce them.
466 This ability might be useful in the design and development of PUFs to identify design weaknesses and correct
467 them before production.

468 It was also shown that the basic idea behind CFD can be extended to produce a new type of machine learning
469 algorithm. CFD identifies and measures differences between two data sets using attribute value combinations,
470 and this approach lends itself naturally to identifying instances in classification problems. An instance that is
471 very similar to others of a particular class is likely to be a member of that class. This paper shows that the
472 accuracy of this CFD approach to classification problems is comparable to the accuracy of well-known
473 algorithms across a variety of problem types. Further research is planned to investigate developing this method
474 into a practical approach for classification problems. In previous work, the authors have used the concept of
475 unique or distinguishing combinations for explainability in AI/ML systems [23][28], so there may be effective
476 methods for combining the CFD method for classification with explainability.

477

References

478 [1] Kuhn, D. R., Mendoza, I. D., Kacker, R. N., & Lei, Y. (2013, March). Combinatorial coverage measurement concepts
 479 and applications. In *2013 IEEE Sixth International Conference on Software Testing, Verification and Validation*
 480 *Workshops* (pp. 352-361). IEEE.
 481 [2] Mendoza, I. D., Kuhn, D. R., Kacker, R. N., & Lei, Y. (2013, October). CCM: A tool for measuring combinatorial
 482 coverage of system state space. In *2013 ACM/IEEE International Symposium on Empirical Software Engineering and*
 483 *Measurement* (pp. 291-291). IEEE.
 484 [3] Kuhn, D.R., Kacker, R.N. and Lei, Y., 2010. Practical combinatorial testing. *NIST special Publication, 800(142)*,
 485 p.142.
 486 [4] Kuhn, D. R., Kacker, R. N., & Lei, Y. (2015). Combinatorial coverage as an aspect of test quality. *CrossTalk*, 28(2),
 487 19-23.
 488 [5] Z. Ratliff, R.Kuhn, R. Kacker, Y.Lei, K. Trivedi, The Relationship Between Software Bug Type and Number of Factors
 489 Involved in Failures, submitted to International Workshop Combinatorial Testing, 2016.
 490 [6] Li, X., Gao, R., Wong, W.E., Yang, C. and Li, D., Applying combinatorial testing in industrial settings. In *2016 IEEE*
 491 *Intl Conf on Software Quality, Reliability and Security (QRS)* (pp. 53-60).
 492 [7] Fifo, M., Enoiu, E., & Afzal, W. (2019, April). On measuring combinatorial coverage of manually created test cases
 493 for industrial software. In *2019 IEEE International Conference on Software Testing, Verification and Validation*
 494 *Workshops (ICSTW)* (pp. 264-267). IEEE.
 495 [8] Smith, R., Jarman, D., Bellows, J., Kuhn, R., Kacker, R., & Simos, D. (2019, April). Measuring Combinatorial
 496 Coverage at Adobe. In *2019 IEEE International Conference on Software Testing, Verification and Validation*
 497 *Workshops (ICSTW)* (pp. 194-197). IEEE.
 498 [9] Mayo, Q., Michaels, R., & Bryce, R. (2014, March). Test suite reduction by combinatorial-based coverage of event
 499 sequences. In *2014 IEEE Seventh International Conference on Software Testing, Verification and Validation*
 500 *Workshops*(pp. 128-132). IEEE.
 501 [10] Morgan, J. (2018). Combinatorial testing: an approach to systems and software testing based on covering
 502 arrays. *Analytic Methods in Systems and Software Testing*, 131-158.
 503 [11] Ozcan, M. (2017, March). Applications of practical combinatorial testing methods at siemens industry inc., building
 504 technologies division. In *2017 IEEE International Conference on Software Testing, Verification and Validation*
 505 *Workshops (ICSTW)* (pp. 208-215). IEEE.
 506 [12] Chandrasekaran, J., Lei, Y., Kacker, R., & Kuhn, D. R. (2021, April). A Combinatorial Approach to Explaining Image
 507 Classifiers. In *2021 IEEE International Conference on Software Testing, Verification and Validation Workshops*
 508 *(ICSTW)* (pp. 35-43). IEEE.
 509 [13] Kuhn, R., Raunak, M. S., & Kacker, R. (2021). *Combinatorial Coverage Difference Measurement (Draft)*. National
 510 Institute of Standards and Technology.
 511 [14] Vijayakumar, A., Patil, V. C., Prado, C. B., & Kundu, S. (2016, May). Machine learning resistant strong PUF: Possible
 512 or a pipe dream? In *2016 IEEE international symposium on hardware oriented security and trust (HOST)* (pp. 19-24).
 513 IEEE.
 514 [15] Ghandehari, L. S., Chandrasekaran, J., Lei, Y., Kacker, R., & Kuhn, D. R. (2015, April). BEN: A Combinatorial
 515 Testing-based Fault Localization Tool. In *Software Testing, Verification and Validation Workshops (ICSTW), 2015*
 516 *IEEE Eighth International Conference on* (pp. 1-4). IEEE.
 517 [16] Herder, C., Yu, M. D., Koushanfar, F., & Devadas, S. (2014). Physical unclonable functions and applications: A
 518 tutorial. *Proceedings of the IEEE*, 102(8), 1126-1141.
 519 [17] Witten, I. H., & Frank, E. (2002). Data mining: practical machine learning tools and techniques with Java
 520 implementations. *Acm Sigmod Record*, 31(1), 76-77.
 521 [18] Majzoobi, M., Koushanfar, F., Potkonjak, M.: Testing techniques for hardware security. In: Test Conference, 2008.
 522 ITC 2008. IEEE International, pp. 1{10 (2008)
 523 [19] D.R. Kuhn, D.R. Wallace, A.M. Gallo, Jr., Software Fault Interactions and Implications for Software Testing, IEEE
 524 Transactions on Software Engineering, vol. 30, no. 6, June 2004, pp. 418-421. Comment: Investigates interaction level
 525 required to trigger faults in a large distributed database system.
 526 [20] D.R. Kuhn and M.J. Reilly, An Investigation of the Applicability of Design of Experiments to Software Testing, 27th
 527 Annual NASA Goddard/IEEE Software Engineering Workshop (SEW '02), Greenbelt, Maryland, December 5-6, 2002,
 528 pp. 91-95

- 529 [21] D. R. Kuhn, V. Okun, Pseudo-exhaustive Testing for Software, 30th Annual IEEE/NASA Software Engineering
530 Workshop (SEW-30), Columbia, Maryland, April 24-28, 2006, pp. 153-158
- 531 [22] Cotroneo, D., Pietrantuono, R., Russo, S., & Trivedi, K. (2016). How do bugs surface? A comprehensive study on the
532 characteristics of software bugs manifestation. *J. Systems and Software*, 113, 27-43.
- 533 [23] R. Kuhn, R. Kacker, An Application of Combinatorial Methods for Explainability in Artificial Intelligence and Machine
534 Learning. *NIST Cybersecurity Whitepaper*, May 22, 2019.
- 535 [24] DR Kuhn, R Kacker, Y Lei, D Simos, "Combinatorial Methods for Explainable AI", *Intl Workshop on Combinatorial*
536 *Testing*, Porto, Portugal, March 23-27, 2020.
- 537 [25] Simos, D. E., Kleine, K., Voyiatzis, A. G., Kuhn, R., & Kacker, R. (2016, August). Tls cipher suites recommendations:
538 A combinatorial coverage measurement approach. In *2016 IEEE International Conference on Software Quality,*
539 *Reliability and Security (QRS)* (pp. 69-73). IEEE.
- 540 [26] Laleh Sh Ghandehari, Yu Lei, Raghu Kacker, Richard Kuhn, Tao Xie, and David Kung. A combinatorial testing-based
541 approach to fault localization. *IEEE Transactions on Software Engineering*, 46(6):616-645, 2018.
- 542 [27] Lanus, E., Freeman, L. J., Kuhn, D. R., & Kacker, R. N. (2021, April). Combinatorial Testing Metrics for Machine
543 Learning. In *2021 IEEE International Conference on Software Testing, Verification and Validation Workshops*
544 *(ICSTW)* (pp. 81-84). IEEE.
- 545 [28] Kampel, L., Simos, D. E., Kuhn, D. R., & Kacker, R. N. (2021). An exploration of combinatorial testing-based
546 approaches to fault localization for explainable AI. *Annals of Mathematics and Artificial Intelligence*, 1-14.
- 547 [29] Y. Hori, H. Kang, T. Katashita and A. Satoh, Pseudo-LFSR PUF: A Compact, Efficient and Reliable Physical
548 Unclonable Function, *2011 International Conference on Reconfigurable Computing and FPGAs*, 2011, pp. 223-228,
549 doi: 10.1109/ReConFig.2011.72.
- 550 [30] U. Ruhrmair, F. Sehnke, J. Solter, G. Dror, S. Devadas, and J. Schmidhuber, Modeling Attacks on Physical Unclonable
551 Functions. *2010. Proc. of the 17th ACM Conference on Computer and Communications Security (CCS '10) ACM*. 237-
552 249. <https://doi.org/10.1145/1866307.1866335>
- 553 [31] R. Kumar and W. Bursleson. 2014. On design of a highly secure PUF based on non-linear current mirrors. In *2014 IEEE*
554 *International Symposium on Hardware Oriented Security and Trust (HOST)*. 38-43. [https://doi.org/10.1109/HST.2014.](https://doi.org/10.1109/HST.2014.6855565)
555 [6855565](https://doi.org/10.1109/HST.2014.6855565)
- 556 [32] Shah, Nimesh, et al. "A 0.16 pj/bit recurrent neural network based PUF for enhanced machine learning attack resistance."
557 *Proceedings of the 24th Asia and South Pacific Design Automation Conference*. 2019.

558

559

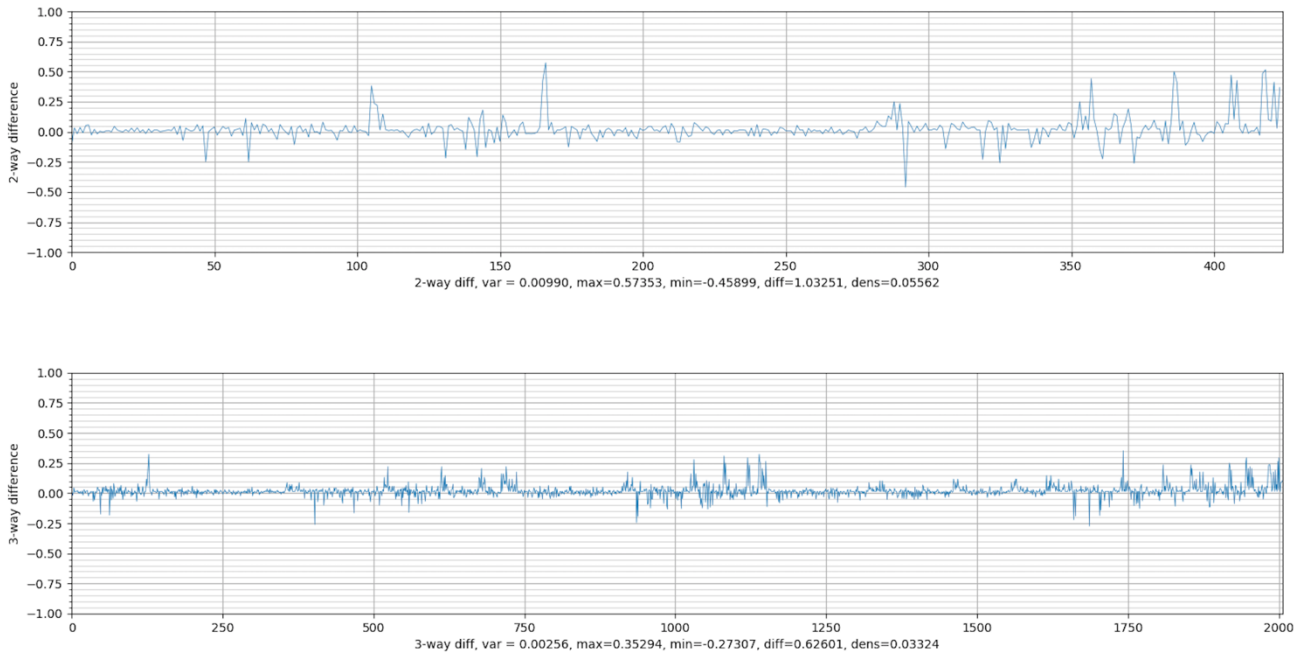
560

561 **Appendix A—Difference Graphs of Classification Problems**

562 This section presents examples of typical machine learning classification problems taken from the UCI
 563 Machine Learning Repository (<https://archive.ics.uci.edu/ml>) or from Kaggle (<https://www.kaggle.com>). Each
 564 example includes the data source, associated publication, and results from the tools described in this paper.

565 **Bcanc** - <https://archive.ics.uci.edu/ml/datasets/Breast+Cancer>

566 Michalski,R.S., Mozetic,I., Hong,J., & Lavrac,N. (1986). The Multi-Purpose Incremental Learning System
 567 AQ15 and its Testing Application to Three Medical Domains. *Proceedings of the Fifth National Conference*
 568 *on Artificial Intelligence*, 1041-1045, Philadelphia, PA: Morgan Kaufmann.



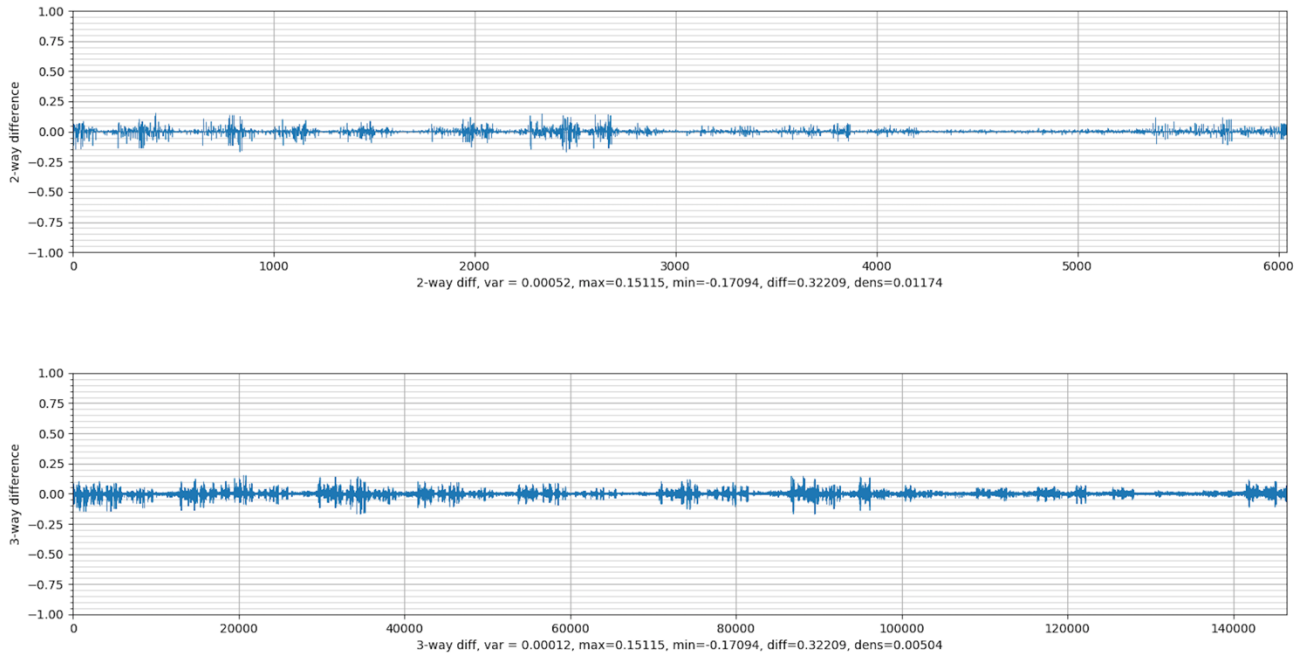
569
 570 **Figure 9. Breast cancer data frequency differences.**

571 CFD results:
 572 == confusion matrix 4-way ==
 573 | C | N <- predicted
 574 C | 75 | 0
 575 N | 3 | 21
 576 =====
 577 Accuracy: 0.970
 578

579 CFDw results:
 580 == confusion matrix 4-way ==
 581 | C | N <- predicted
 582 C | 24 | 0
 583 N | 2 | 73
 584 =====
 585 Accuracy: 0.980
 586 =====
 587

588 **Coupon** - <https://www.kaggle.com/mathurinache/invehicle-coupon-recommendation>

589 Wang, Tong, Cynthia Rudin, Finale Doshi-Velez, Yimin Liu, Erica Klampfl, and Perry MacNeille. 'A
590 Bayesian framework for learning rule sets for interpretable classification.' The Journal of Machine Learning
591 Research 18, no. 1 (2017): 2357-2393.



592
593 **Figure 10. Coupon data frequency differences.**

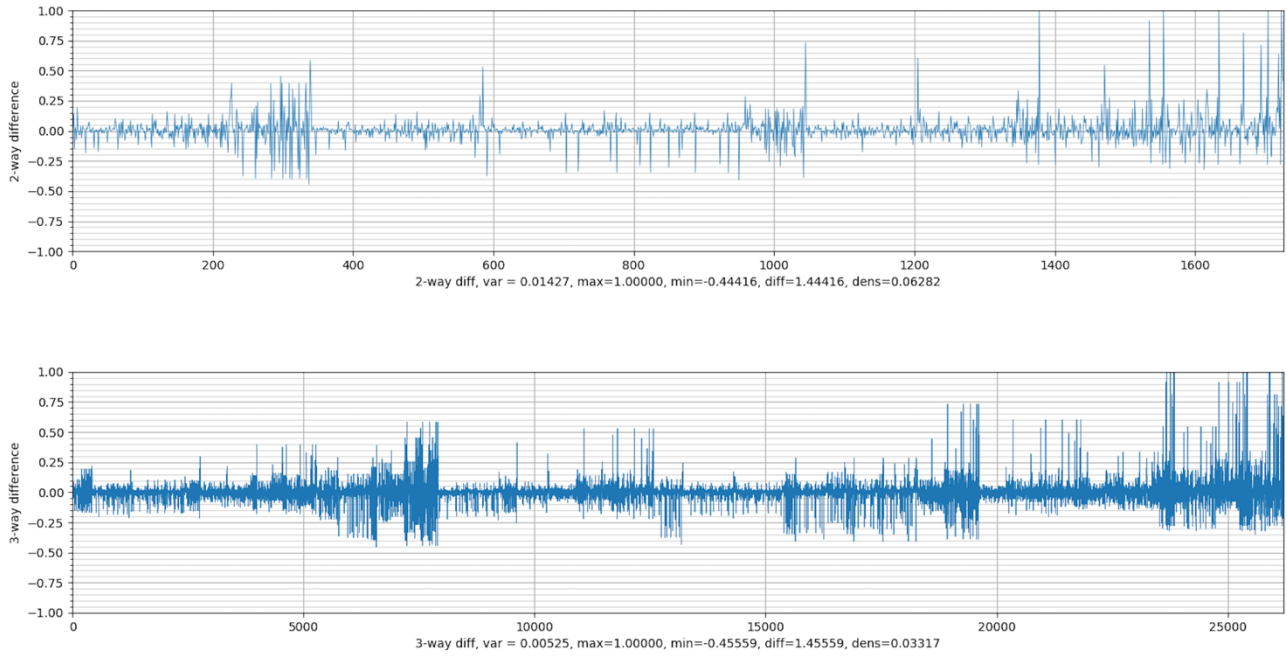
```
594 == confusion matrix 4-way ==  
595 | C | N <- predicted  
596 C | 1931 | 521  
597 N | 661 | 1201  
598 =====  
599 Accuracy: 0.726  
600 =====
```

601

602

603
604
605
606
607

Credit - https://archive.ics.uci.edu/ml/citation_policy.html
Dua, D. and Graff, C. (2019). UCI Machine Learning Repository [<http://archive.ics.uci.edu/ml>]. Irvine, CA: University of California, School of Information and Computer Science.



608

Figure 11. German credit check data frequency differences.

609

610

```
== confusion matrix 4-way ==  
 |      C |      N  <- predicted  
C |      10 |      3  
N |      0 |     328  
=====
```

615

```
Accuracy: 0.991  
=====
```

617

618

619

```
CFDw results:
```

620

```
== confusion matrix 4-way ==  
 |      C |      N  <- predicted  
C |     293 |     35  
N |      0 |     13  
=====
```

622

```
Accuracy: 0.897  
=====
```

623

624

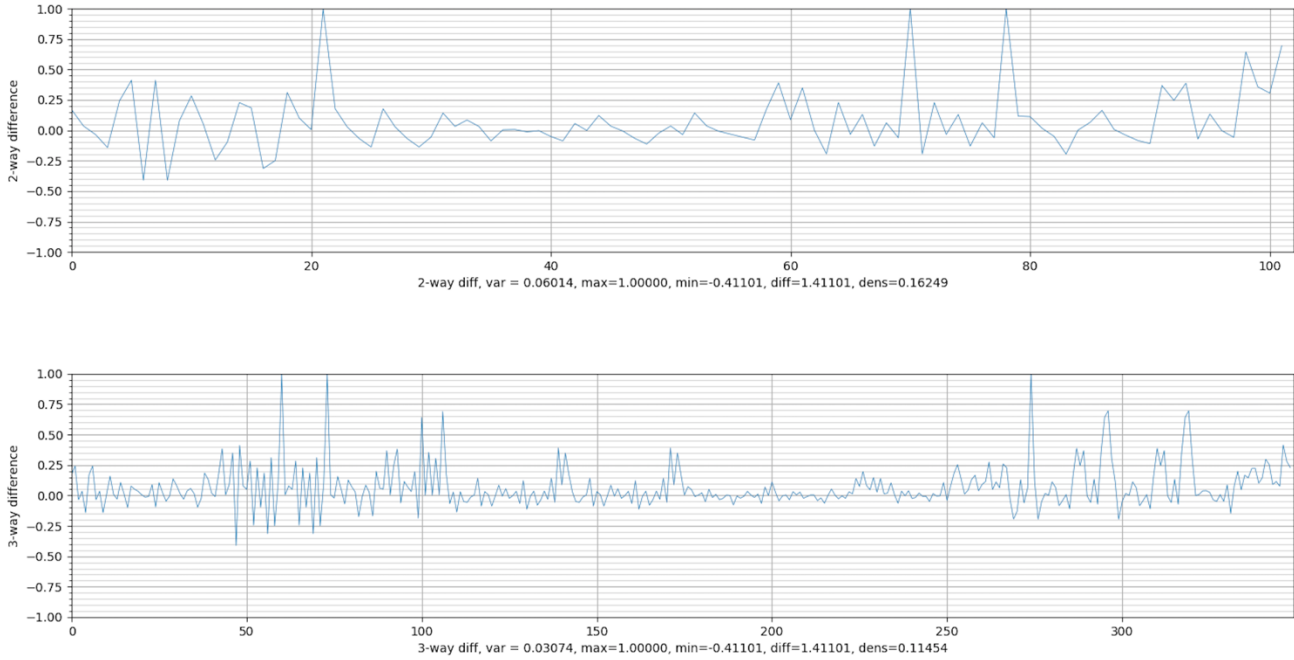
625

626

627

628 **Diab** - <https://archive.ics.uci.edu/ml/datasets/diabetes>

629 Smith, J.W., Everhart, J.E., Dickson, W.C., Knowler, W.C., Johannes, R.S. (1988). Using the ADAP learning
630 algorithm to forecast the onset of diabetes mellitus. *Proceedings of the Symposium on Computer Applications*
631 *and Medical Care* (pp. 261--265). IEEE.



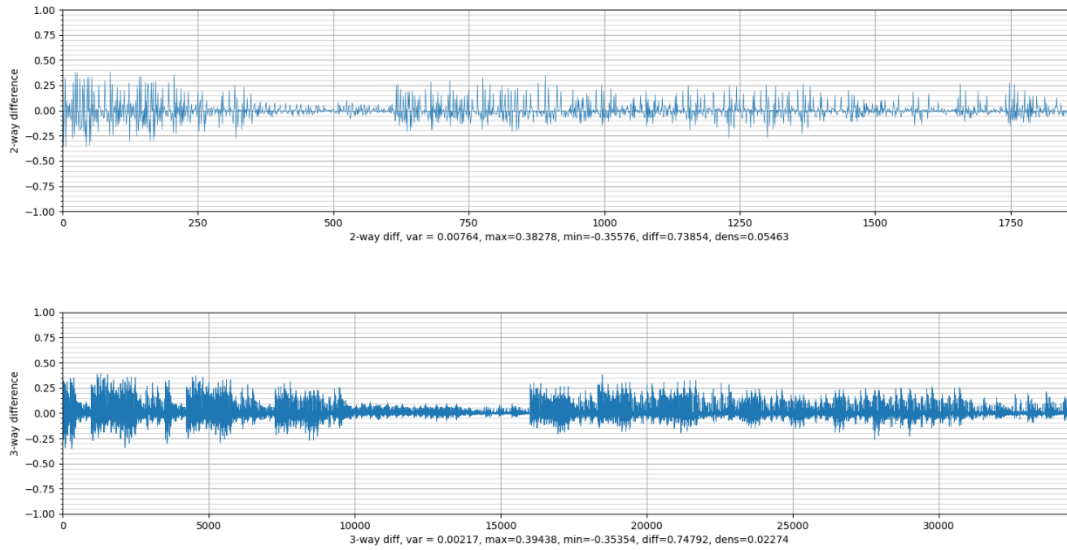
632
633 **Figure 12. Diabetes data frequency differences.**

```
634 CFD results:  
635 == confusion matrix 4-way ==  
636 | C | N <- predicted  
637 C | 124 | 1  
638 N | 1 | 136  
639 =====  
640 Accuracy: 0.992  
641  
642 CFDw results:  
643 == confusion matrix 4-way ==  
644 | C | N <- predicted  
645 C | 125 | 0  
646 N | 1 | 136  
647 =====  
648 Accuracy: 0.996  
649 =====
```

650

651 **Heart2** - <https://github.com/doguilmak/Heart-Diseaseor-Attack-Classification>

652 Large set of data containing 253,681 instances, with 23,893 heart disease or attack, and the rest healthy. To
 653 make instance sets equal size, a random set of 23,893 disease/attack instances were extracted.



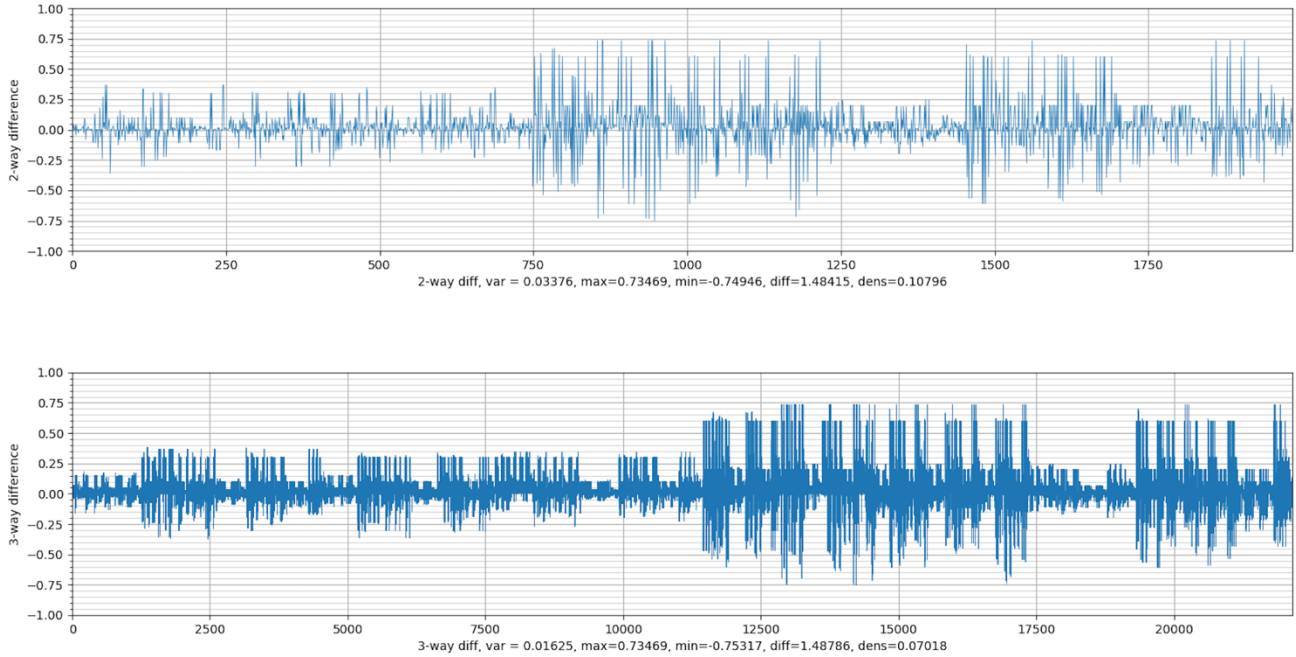
654
 655 **Figure 13. Heart disease data frequency differences.**

```

656 == confusion matrix 2-way ==
657 |      C |      N  <- predicted
658 C |  6254 |  1870
659 N |  2472 |  5652
660 =====
661 Accuracy 2-way = 0.733, SD_2 = 0.08709, dt = 1.046
662
663 == confusion matrix 3-way ==
664 |      C |      N  <- predicted
665 C |  6017 |  2107
666 N |  1950 |  6174
667 =====
668 Accuracy 3-way = 0.750, SD_3 = 0.04643, dt = 1.046
669 == confusion matrix 4-way ==
670 |      C |      N  <- predicted
671 C |  5905 |  2219
672 N |  1764 |  6360
673 =====
674 Accuracy 4-way = 0.755, dt = 1.046
675
676 == confusion matrix 5-way ==
677 |      C |      N  <- predicted
678 C |  5859 |  2265
679 N |  1991 |  6133
680 =====
681 Accuracy 5-way = 0.738, dt = 1.046
682 =====
683
    
```

684 **Mush** - <https://archive.ics.uci.edu/ml/datasets/Mushroom>

685 Schlimmer, J.S. (1987). Concept Acquisition Through Representational Adjustment (Technical Report 87-19).
686 Doctoral dissertation, Department of Information and Computer Science, University of California, Irvine.



687
688 **Figure 14. Edible mushroom data frequency differences.**

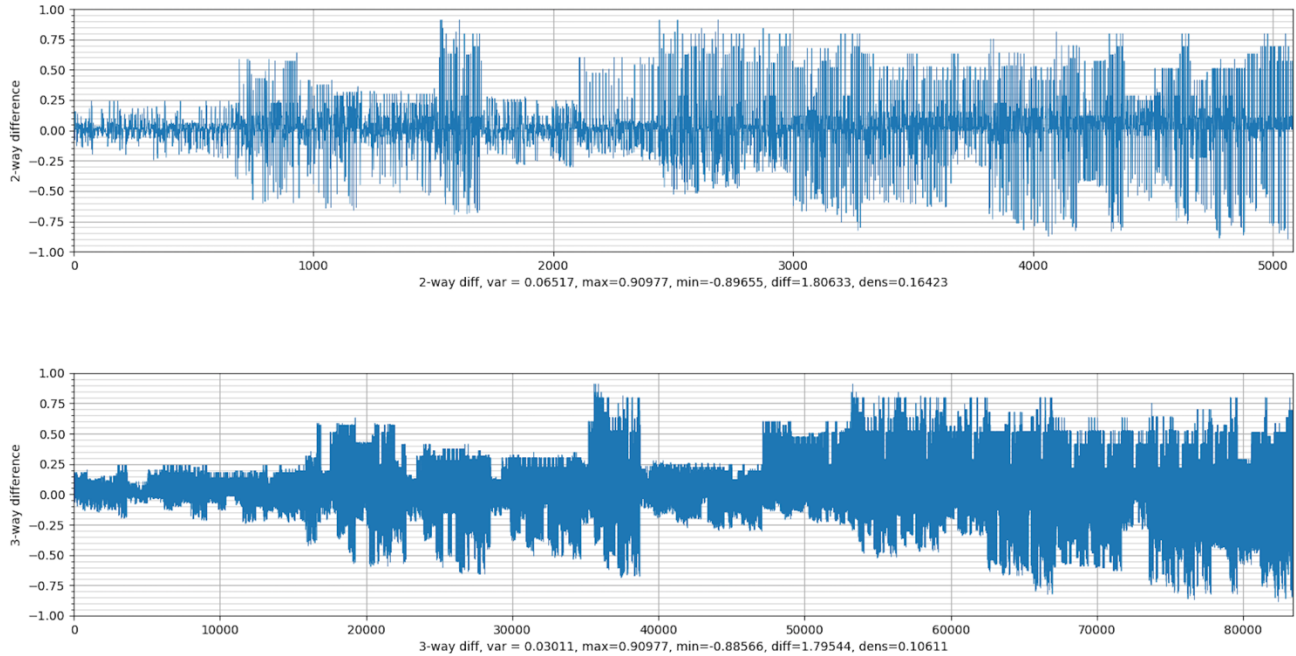
689 CFD results:
690 == confusion matrix 4-way ==
691 | C | N <- predicted
692 C | 725 | 9
693 N | 58 | 1128
694 =====
695 Accuracy: 0.965
696

697 CFDw results:
698 == confusion matrix 4-way ==
699 | C | N <- predicted
700 C | 553 | 181
701 N | 0 | 1186
702 =====
703 Accuracy: 0.906
704 =====
705

706

707 Soyb - <https://archive.ics.uci.edu/ml/datasets/Soybean+%28Large%29>

708 R.S. Michalski and R.L. Chilausky. "Learning by Being Told and Learning from Examples: An Experimental
709 Comparison of the Two Methods of Knowledge Acquisition in the Context of Developing an Expert System
710 for Soybean Disease Diagnosis", *International Journal of Policy Analysis and Information Systems*, Vol. 4,
711 No. 2, 1980.



712

713

Figure 15. Soybean disease data frequency differences.

714

```
CFD results:  
== confusion matrix 4-way ==  
   |      C      |      N      |<- predicted  
C  |      42     |      4     |  
N  |      0      |     188    |  
=====
```

719

Accuracy: 0.983

721

722

```
CFDw results:  
== confusion matrix 4-way ==  
   |      C      |      N      |<- predicted  
C  |      41     |      5     |  
N  |      0      |     188    |  
=====
```

727

Accuracy: 0.979

729

730